24. Jampol LM, Shankle J, Schroeder R, Tornambe P, Spaide RF, Hee MR. Diagnostic and therapeutic challenges. Retina 2006;26(9):1072–1076.
25. Margolis R, Mukkamala SK, Jampol LM, et al. The expanded spectrum of focal choroidal excavation. Arch Ophthalmol 2011;129(10):1320–1325.
26. Wakabayashi Y, Nishimura A, Higashide T, Ijiri S, Sugiyama K. Unilateral choroidal excavation in the macula detected by spectral-domain optical coherence tomography. Acta Ophthalmol 2010;88(3):e87–91.
27. Naumann GOH, Apple DJ. Pathology of the eye. New York: Springer-Verlag; 1986.
28. Dichtl A, Jonas JB, Naumann GO. Histomorphometry of the optic disc in highly myopic eyes with absolute secondary angle closure glaucoma. Br J Ophthalmol 1998;82(3):286–289.
29. Gopal L, Khan B, Jain S, Prakash VS. A clinical and optical coherence tomography study of the margins of choroidal colobomas. Ophthalmology 2007;114(3):571–580.
30. Baba T, Ohno-Matsui K, Futagami S, et al. Prevalence and characteristics of foveal retinal detachment without macular hole in high myopia. Am J Ophthalmol 2003;135(3):338–342.
31. Chen L, Wang K, Esmaili DD, Xu G. Rhegmatogenous retinal detachment due to paravascular linear retinal breaks over patchy chorioretinal atrophy in pathologic myopia. Arch Ophthalmol 2010;128(12):1551–1554.
32. Gaucher D, Erginay A, Lecleire-Collet A, et al. Dome-shaped macula in eyes with myopic posterior staphyloma. Am J Ophthalmol 2008;145(5):909–914.
33. Imamura Y, Iida T, Maruko I, Zweifel SA, Spaide RF. Enhanced depth imaging optical coherence tomography of the sclera in dome-shaped macula. Am J Ophthalmol 2011;151(2):297–302.
34. Curtin BJ. The posterior staphyloma of pathologic myopia. Trans Am Ophthalmol Soc 1977;75:67–86.

AJO History of Ophthalmology Series

Joaquin Rodrigo

Among those remarkable people who are blind since childhood, but who go on to accomplish great things, should be recognized the Spanish composer, Joaquín Rodrigo (1901-1999). Blinded by diphtheria at age 3, he became a virtuoso pianist and composer of classical music, elevating the classical guitar into the concert repertoire with such popular pieces as the *Concierto de Aranjuez*, and the *Fantasía para un gentilhombre*. Composed in Braille, his music had to be transcribed before it could be performed. In 1991, the King of Spain awarded him the noble, hereditary, and inspired title of Marquis of the Gardens of Aranjuez.

Submitted by Ron Fishman of the Cogan Ophthalmic History Society

Epilepsy Research (2012) xxx, xxx–xxx

ELSEVIER

journal homepage: www.elsevier.com/locate/epilepsyres

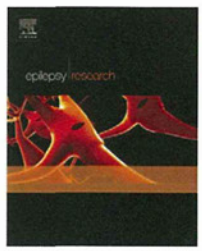

Altered extrafocal iomazenil activity in mesial temporal lobe epilepsy

Koichi Hosomi[a,b], Haruhiko Kishima[a,*], Satoru Oshino[a], Masayuki Hirata[a], Naoki Tani[a,c], Tomoyuki Maruo[a], Hui Ming Khoo[a], Eku Shimosegawa[d], Jun Hatazawa[d], Amami Kato[e], Toshiki Yoshimine[a]

[a] *Department of Neurosurgery, Osaka University Graduate School of Medicine, Osaka, Japan*
[b] *Department of Neuromodulation and Neurosurgery, Office for University-Industry Collaboration, Osaka University, Osaka, Japan*
[c] *Department of Neurosurgery, Otemae Hospital, Osaka, Japan*
[d] *Department of Nuclear Medicine and Tracer Kinetics, Osaka University Graduate School of Medicine, Osaka, Japan*
[e] *Department of Neurosurgery, Kinki University Faculty of Medicine, Osaka, Japan*

Received 7 February 2012; received in revised form 6 June 2012; accepted 3 July 2012

KEYWORDS
Iomazenil SPECT;
Interhemispheric asymmetry;
Mesial temporal lobe epilepsy;
Central benzodiazepine receptor

Summary To investigate involvement of extrafocal regions in mesial temporal lobe epilepsy (MTLE), we retrospectively explored abnormalities in distribution of iomazenil (IMZ) activity by identifying interhemispheric asymmetry on IMZ-SPECT images of patients with MTLE. Fourteen MTLE patients in whom a good surgical outcome was achieved were included in the study. Voxel-based (VB) analysis and volume-of-interest (VOI) analysis with predefined VOIs were applied to compare IMZ binding between the hemispheres ipsilateral and contralateral to the epileptic focus. VB analysis showed significant decreases in iomazenil binding not only in the ipsilateral anterior temporal lobe including the mesial temporal structures but also in the ipsilateral extratemporal region including the insula, putamen, and medial occipital lobe. VOI analysis showed similar significant decreases in the ipsilateral parahippocampal gyrus, amygdala, putamen, lateral temporal lobe, and lateral occipital lobe. Results of the SPECT analyses suggest that decreased or dysfunctional IMZ activity extends from the mesial temporal lobe to the ipsilateral extrafocal region in patients with MTLE.

Introduction

Mesial temporal lobe epilepsy (MTLE) is one of the main types of partial-onset epilepsy and is characterized by seizures that originate in the hippocampus, amygdala, or other mesial structures in the temporal lobe. Several studies have shown that the histologic, morphologic, and functional brain abnormalities associated with MTLE extend

* Corresponding author at: Department of Neurosurgery, Osaka University Graduate School of Medicine, 2-2 Yamadaoka, Suita, Osaka 565-0871, Japan. Tel.: +81 6 6879 3652; fax: +81 6 6879 3659.
E-mail address: hkishima@nsurg.med.osaka-u.ac.jp (H. Kishima).

0920-1211/$ – see front matter © 2012 Elsevier B.V. All rights reserved.
http://dx.doi.org/10.1016/j.eplepsyres.2012.07.001

beyond the mesial temporal lobe to regions adjacent to the hippocampus as well as extratemporal structures (Henry et al., 1990; Arnold et al., 1996; Dupont et al., 1998; Hammers et al., 2001; Bouilleret et al., 2002; Cendes et al., 2005; Didelot et al., 2010). These abnormalities have been evaluated in resected specimens, at autopsy, by magnetic resonance imaging (MRI), and by nuclear imaging.

Central benzodiazepine receptor (cBZR) labeling is used in nuclear imaging to identify epileptic foci. Expression of cBZR, a component of the gamma-aminobutyric acid (GABA)-A receptor complex, can represent inhibitory function of the brain (Umeoka et al., 2007). A histological study of brain tissues obtained from animal epilepsy models revealed decreased cBZR density in the epileptic foci (Kurokawa et al., 1994). Examination of slice preparations of human brain tissues taken from epileptic foci also revealed decreased cBZR density (Johnson et al., 1992).

^{11}C-flumazenil (FMZ) is a selective cBZR antagonist used as a positron emission tomography (PET) tracer, and ^{123}I-iomazenil (IMZ) is a selective cBZR agonist used in single photon emission computed tomography (SPECT); both have been used to detect epileptic foci. IMZ-SPECT has come into widespread use for presurgical detection of epileptic foci (Kaneko et al., 2006; Umeoka et al., 2007) because of the availability of both tracer and gamma camera. However, few IMZ-SPECT studies have examined extrafocal alterations in the whole brain of patients with MTLE, except for studies examining the diagnostic value of IMZ-SPECT (Tanaka et al., 1997; Kaneko et al., 2006; Umeoka et al., 2007). We conducted a retrospective study of IMZ-SPECT images to explore abnormalities, i.e., interhemispheric asymmetry, in IMZ activity in patients with MTLE. We used two different analytical methods: voxel-based (VB) analysis with statistical parametric mapping (SPM) and predefined volume-of-interest (VOI) analysis with three-dimensional stereotactic surface projection (3D-SSP). Both methods are excellent in terms of reproducibility and objectivity, owing to automatic spatial normalization and statistical analysis of the whole brain (Minoshima et al., 1994; Friston et al., 1995a,b; Minoshima et al., 1995; Hosoda et al., 2005; Takada et al., 2006).

Methods

Patients

Fourteen patients with refractory MTLE who were treated surgically at our hospital between 2004 and 2010 and in whom a satisfactory surgical outcome, i.e., Engel's class I or II (Engel et al., 1993), was achieved were included in the study (11 females, 3 males; median age at seizure onset: 7.5 years, range: 1–24 years; median age at surgery: 19 years, range: 13–46 years; median follow-up time after surgery: 57 months, range: 12–85 months). All 14 patients had undergone preoperative interictal IMZ-SPECT at our hospital while receiving antiepileptic medications. All antiepileptic medications, including benzodiazepines (clonazepam, 2–6 mg daily; clobazam, 10–30 mg daily), were continued. Clinical characteristics of the 14 patients are summarized in Table 1.

The preoperative diagnoses of MTLE were based on clinical history, semiology, and MRI, interictal ^{18}F-fluorodeoxyglucose (FDG) PET, magnetoencephalographic monitoring, and long-term video scalp electroencephalography (EEG) findings. All patients suffered daily to monthly seizures despite appropriate medical treatment with several antiepileptic drugs for more than 1 year after seizure onset. Most patients showed typical MTLE semiology, i.e., abdominal aura ($n = 12$), automatism ($n = 10$), dystonic posturing ($n = 4$). Brain MRI revealed ipsilateral hippocampal atrophy in 10 patients and signal intensity changes in the ipsilateral hippocampus on T2-weighted and/or FLAIR images in 9 of these 10 patients. MRI revealed a parahippocampal lesion in one patient (Patient 1). No MRI abnormalities were seen in the remaining three patients.

All surgeries had been comprehensively planned on the basis of preoperative examinations with ($n = 6$) or without ($n = 8$) invasive EEG recordings and were guided by intraoperative electrocorticography. Selective amygdalohippocampectomy was performed in 13 patients. Outcomes more than 1 year after surgery were regarded corresponding to Engel's class I (Engel et al., 1993), except in one case. Histopathologic examination of resected tissues revealed hippocampal sclerosis ($n = 10$), cortical dysplasia of the parahippocampal gyrus ($n = 2$), gliosis ($n = 1$), and ganglioglioma ($n = 1$), confirming that the epileptic foci were located in mesial temporal structures and that the diagnosis of MTLE was accurate in all cases.

Acquisition of SPECT images

IMZ-SPECT had been performed in all 14 patients in the interictal state; all were taking antiepileptic medications. Delayed images, which reflect mainly tracer binding to cBZR (Beer et al., 1990; Schubiger et al., 1991; Tanaka et al., 1997), were acquired 3 h after intravenous injection of 167 MBq ^{123}I-IMZ. A four-headed gamma camera (Gamma View SPECT 2000H, Hitachi, Tokyo, Japan) equipped with low-energy middle-resolution parallel-hole collimators (64 × 64 matrix) was used (intrinsic spatial resolution, 3.1 mm full width at half maximum, useful field of view) (Kimura et al., 1990). Raw data were obtained at 20 s per step over a 360° rotation. Transaxial images (voxel size, 4 mm × 4 mm × 4 mm) were reconstructed with a Butterworth filter (cut-off frequency 0.20 cycle/pixel, order 10) and attenuation correction (Chang method, attenuation coefficient: 0.08/cm). Qualitative images were created, and the hemispheres ipsilateral and contralateral to the epileptic focus were compared.

VB analysis of IMZ-SPECT images

Because the epileptic focus was left-sided in six patients and right-sided in eight patients, the IMZ-SPECT images obtained from the six patients with left MTLE were left-right flipped before preprocessing (MRIcro; http://www.sph.sc.edu/comd/rorden/mricro.html) to align the epileptogenic zone on the right side, as previously described (Kim et al., 2003; Hammers et al., 2008). These alignments let all 14 cases be statistically analyzed together.

Please cite this article in press as: Hosomi, K., et al., Altered extrafocal iomazenil activity in mesial temporal lobe epilepsy. Epilepsy Res. (2012), http://dx.doi.org/10.1016/j.eplepsyres.2012.07.001

Table 1 Patients' clinical characteristics.

Patient	Age (y)	Sex	Age at seizure onset (y)	Seizures	Medication (s)	Laterality	MRI findings	Histology	Scalp EEG	IMZ-SPECT: decreases	FDG-PET: decreases	Invasive EEG	Outcome[a]
1	14	F	1	Weekly SPS and CPS	CBZ, CLB, CZP	Rt	Lesion (Rt PHG)	Ganglioglioma	Rt T (interictal) SP2 (ictal)	Rt m-T	Rt m-T	–	Ia
2	30	F	8	Weekly SPS, Monthly CPS	CBZ, CLB, CZP	Rt	Rt HA, HI	HS	Rt FT (interictal)	–	Rt m-T	Rt m-T (ictal)	Ia
3	28	F	19	Monthly CPS	CBZ	Lt	Lt HA, HI	HS	F3, T3 (interictal) Lt (ictal)	Lt T	Lt T	Lt tip-m-T (ictal)	Ia
4	21	M	4	Daily SPS, Monthly CPS and SGS	PHT, VPA	Rt	–	HS	Rt T (interictal)	Rt T	Rt m-T	–	Ia
5	13	F	10	Daily SPS, Weekly CPS	CBZ	Rt	–	CD	Rt FT (interictal) Rt FT (ictal)	Rt TP, Lt m-T	Rt T, Rt F, Rt O	Rt m-T (ictal)	Ia
6	14	F	11	Weekly SPS and CPS	VPA, ZNS, CLB	Lt	Lt HA, HI	HS	Lt T (interictal) Lt T (ictal)	Lt m-tip-T, Bil m-F	Bil base-T, Bil Thal	–	Ia
7	46	M	24	Monthly SPS	PHT, PB	Rt	–	Gliosis	SP2 (interictal)	Bil T	Rt m-T, Rt l-T	–	Ia
8	19	F	1	Weekly SPS and CPS	ZNS, CZP	Lt	Lt HA, HI	CD	Bil F-C, Lt T (interictal) Lt T (ictal)	Lt m-base-T, Bil F	Lt m-T	Lt m-T (ictal)	IIa
9	17	F	10	Daily CPS	PHT, ZNS, AZA	Lt	Lt HA, HI	HS	Lt FT (ictal)	Lt m-tip-T	Lt m-tip-l-T	–	Ia
10	16	F	2	Weekly CPS, Yearly SGS	VPA, TPM	Lt	Lt HA, HI	HS	T3, SP1 (ictal)	Lt m-T, Lt l-T	Lt m-T	–	Ia
11	33	F	3	Dialy SPS, Monthly CPS	CLB	Rt	Rt HA, HI	HS	F8 (interictal)	Rt m-T	Rt m-T, Rt l-T	–	Ib
12	22	F	7	Weekly CPS	VPA, LTG	Rt	Rt HA, HI	HS	F8, T4, SP2 (interictal) T4 (ictal)	Rt m-T	Rt m-tip-T	Rt base-T (interictal)	Ia
13	16	M	3	Daily CPS, Monthly SGS	LTG, PHT, TPM, ZNS	Lt	Lt HA	HS	F7 (interictal) F7 (ictal)	Lt l-T	Lt m-tip-T	Lt m-T (ictal)	Ia
14	19	F	12	Monthly CPS	CBZ, CLB	Rt	Rt HA, HI	HS	F4 (interictal) Rt FT (ictal)	Rt m-T, Rt l-T	Rt T	–	Ia

y, year; m, month; F, female; M, male; SPS, simple partial seizure; CPS, complex partial seizure; SGS, secondary generalized seizure; CBZ, carbamazepine; CLB, clobazam; CZP, clonazepam; PHT, phenytoin; VPA, valproate; ZNS, zonisamide; PB, phenobarbital; AZA, acetazolamide; TPM, topiramate; LTG, lamotrigine; Lt, left; Rt, right; Bil, bilateral; HA, hippocampal atrophy; HI, hippocampal high signal intensity on T2-weighted and/or FLAIR images; PHG, parahippocampal gyrus; HS, hippocampal sclerosis; CD, cortical dysplasia; T, temporal lobe; SP, sphenoidal electrode; FT, fronto-temporal lobe; TP, temporo-parietal lobe; F, frontal lobe; O, occipital lobe; Thal, thalamus; m-, medial part; base-, basal part; l-, lateral part.

[a] Reported as Engel's classification (Engel et al., 1993).

Please cite this article in press as: Hosomi, K., et al., Altered extrafocal iomazenil activity in mesial temporal lobe epilepsy. Epilepsy Res. (2012), http://dx.doi.org/10.1016/j.eplepsyres.2012.07.001

Spatial preprocessing and statistical analysis of SPECT images were performed with SPM8 (Wellcome Department of Imaging Neuroscience, Institute of Neurology, University College London, London, UK) implemented in MATLAB 7.11.0 (MathWorks Inc., Massachusetts, USA) (Friston et al., 1995a,b; Kugaya et al., 2003; Heinzel et al., 2008). SPM8 provides for statistical parametric mapping of neuroimaging data. Individual SPECT images were spatially normalized to the standard stereotactic space (voxel size, 2 mm × 2 mm × 2 mm) of the Montreal Neurological Institute (MNI) brain by applying a symmetrical SPECT template created from an asymmetrical template provided in SPM8 (Didelot et al., 2010). This spatial normalization was performed by using the optimum 12-parameter affine transformation and nonlinear deformations. The accuracy of spatial normalization was visually confirmed on the display by comparing the normalized images to the template. The normalized images were smoothed with a 12-mm FWHM Gaussian filter to increase the signal-to-noise ratio. Global nuisance effects were removed by including the global covariate as a nuisance effect in the general linear model (ANCOVA). Interhemispheric asymmetry was examined in all 14 patients with right or ''flipped right'' MTLE to detect relative decrease and increase in IMZ binding. IMZ binding in the ipsilateral (right) hemisphere was compared (voxel-by-voxel) to that in the contralateral (left) hemisphere, and the difference was analyzed by paired t test with SPM8. Differences in uncorrected voxel levels were considered significant at $p < 0.001$, and those in uncorrected cluster levels were considered significant at $p < 0.05$. One hundred or more contiguous voxels were examined in the ipsilateral (right) hemisphere, including the epileptic focus (Van Bogaert et al., 2000; Kim et al., 2003). Coordinates of interest were converted from MNI space to the Talairach atlas by using the Brett transform (Brett et al., 2002), and areas of interest were localized according to the Talairach atlas (Talairach and Tournoux, 1988).

VOI analysis of IMZ-SPECT images

The automatic VOI analysis toolkit (VOIClassic) included in NEUROSTAT software library (Nihon Medi-Physics Co. Ltd., Tokyo, Japan) was applied to evaluate asymmetry of IMZ binding in each VOI (Hosoda et al., 2005; Takada et al., 2006). The program automatically calculated the average count per voxel in a VOI, which was predefined on the standard stereotactic space of the Talairach atlas covering the whole brain. Each original SPECT image was first stereotactically transformed into a standard 3D surface image by making use of the 3D-SSP in NEUROSTAT (Minoshima et al., 1994, 1995; Ishii et al., 2001). The original images were spatially normalized to the standard stereotactic space according to the Talairach atlas by applying the IMZ-SPECT template provided in NEUROSTAT, and the peak cortical activity within six voxels from the brain surface was projected onto the surface voxels. After accuracy of the spatial normalization was checked, VOIClassic calculated the average count in each of the 37 predefined VOIs on the transformed surface images. The predefined 37 VOIs were provided by VOIClassic software and consisted of the bilateral VOIs listed in Table 3, pons, whole cerebral cortices, and whole brain. For each individual, each average count was divided by the individual total count of the whole cerebellum to correct for global inter-individual differences. The corrected counts of all 14 patients were then compared between the ipsilateral and contralateral sides in each region by paired t test. Values are shown as mean corrected counts ± SD. Differences were considered significant at $p < 0.05$.

Table 2 Areas of significantly decreased iomazenil binding (according to voxel-based analysis).

Area	Peak	Cluster		Talairach coordinates of peaks (x, y, z, mm)/voxel equivalent Z		
		p value	Size (voxels)			
Anterior temporal, Insula, Putamen, Supratemporal		< 0.001	5189			
	Temporal tip (STG, BA38)			45, 10, −28/6.14		(A)
	Medial temporal (Hippocampus, BA28)			20, −13, −15/5.06		(B)
	Lateral temporal (MTG, BA21)			41, −1, −25/4.90		(C)
	Temporal stem			27, 16, −12/4.75	40, 10, −10/4.40	(D)
	Temporal tip (BA36)			36, 2, −36/4.71	27, −3, −34/4.56	(E)
	Insula, Putamen			33, −23, 15/3.86		(F)
	Lateral temporal (STG, BA22)			56, −5, 1/3.73		(G)
	Medial supratemporal plane			43, −30, 16/3.67		(H)
Medial occipital	(Cuneus, BA18)	0.006	173	3, −77, 10/3.95		(I)

STG, superior temporal gyrus; BA, Brodmann's area; MTG, middle temporal gyrus.

Please cite this article in press as: Hosomi, K., et al., Altered extrafocal iomazenil activity in mesial temporal lobe epilepsy. Epilepsy Res. (2012), http://dx.doi.org/10.1016/j.eplepsyres.2012.07.001

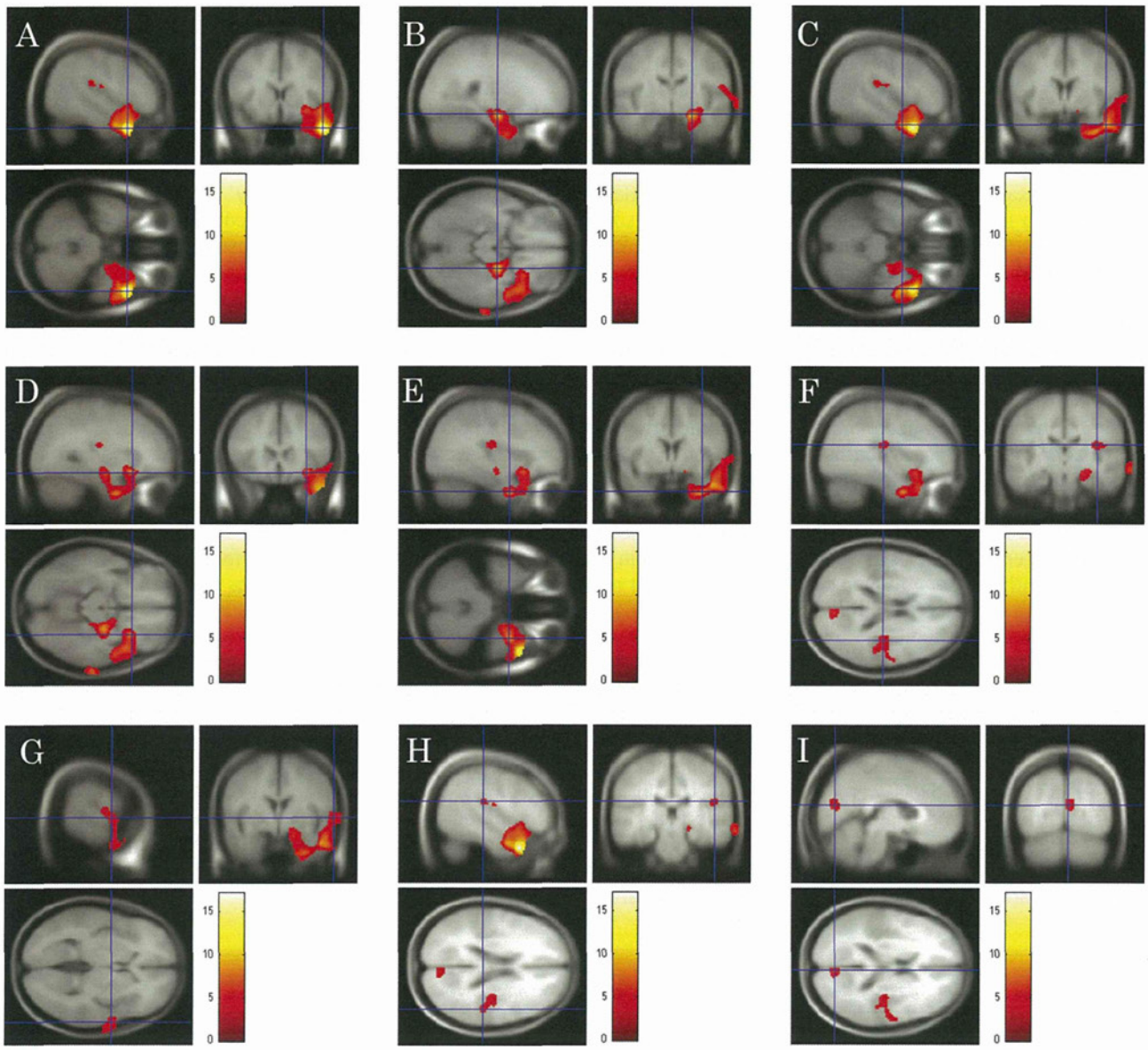

Figure 1 Statistical parametric maps (Z maps) of intensity on normalized images obtained from all 14 patients. Significant decreases in IMZ binding in the hemisphere ipsilateral to the epileptic focus were present in the anterior temporal lobe (A–E, G), the insula, putamen, and supratemporal plane (F, H), and the medial occipital lobe (I). Color bars show the *Z* score scale. Panels A–K correspond to Table 2.

Results

VB analysis of the IMZ-SPECT images from all 14 patients revealed significantly decreased IMZ binding in the following areas of the hemisphere ipsilateral to the epileptic focus: the anterior temporal lobe, insula, putamen, and supratemporal plane (cluster size, 5189 voxels; $p < 0.001$); and the medial occipital lobe (cluster size, 173 voxels; $p = 0.006$). Decreases in the anterior temporal lobe included decreases in the medial, tip, and lateral parts, including the hippocampus. Significant increases in IMZ binding were not seen in the ipsilateral hemisphere (Table 2, Fig. 1).

VOI analysis of the IMZ-SPECT images from all 14 patients revealed significantly decreased IMZ binding in the parahippocampal gyrus and amygdala on the ipsilateral side vs. the contralateral side: 0.620 ± 0.106 vs. 0.714 ± 0.061, $p = 0.004$; 0.660 ± 0.118 vs. 0.762 ± 0.092, $p < 0.001$. Counts were also significantly lower on the ipsilateral side (vs. contralateral side) in the putamen, lateral temporal lobe, and lateral occipital lobe: 0.618 ± 0.108 vs. 0.696 ± 0.146, $p = 0.012$; 1.270 ± 0.084 vs. 1.301 ± 0.083, $p = 0.023$; 1.475 ± 0.108 vs. 1.518 ± 0.137, $p = 0.005$. There were no ipsilateral VOIs with significantly higher counts (Table 3, Fig. 2).

Discussion

This study is the first to document altered IMZ activity in the anterior temporal and extratemporal regions in MTLE

Please cite this article in press as: Hosomi, K., et al., Altered extrafocal iomazenil activity in mesial temporal lobe epilepsy. Epilepsy Res. (2012), http://dx.doi.org/10.1016/j.eplepsyres.2012.07.001

Table 3 Corrected iomazenil counts within each VOI.

VOI	Mean (SD)		*p* value*
	Ipsilateral side	Contralateral side	
Lateral frontal cortex	1.302 (0.099)	1.308 (0.102)	0.475
Lateral temporal cortex	1.270 (0.084)	1.301 (0.083)	0.023*
Lateral parietal cortex	1.411 (0.114)	1.416 (0.110)	0.633
Lateral occipital lobe	1.475 (0.108)	1.518 (0.137)	0.005*
Anterior cingulate cortex	0.932 (0.123)	0.937 (0.122)	0.487
Posterior cingulate cortex	1.131 (0.141)	1.114 (0.128)	0.187
Medial frontal cortex	1.229 (0.106)	1.245 (0.096)	0.195
Medial parietal cortex	1.436 (0.111)	1.407 (0.119)	0.139
Primary sensorimotor cortex	1.365 (0.102)	1.385 (0.119)	0.130
Primary visual cortex	1.851 (0.161)	1.863 (0.167)	0.564
Caudate nucleus	0.469 (0.089)	0.474 (0.090)	0.655
Cerebellar hemisphere	0.936 (0.036)	0.939 (0.033)	0.728
Cerebellar vermis	1.170 (0.099)	1.180 (0.087)	0.561
Putamen	0.618 (0.108)	0.696 (0.146)	0.012*
Parahippocampal gyrus	0.620 (0.106)	0.714 (0.061)	0.004*
Amygdala	0.660 (0.118)	0.762 (0.092)	<0.001*
Thalamus	0.344 (0.074)	0.338 (0.101)	0.706

VOI, volume of interest predefined on the standard stereotactic space of the Talairach atlas. Sides are ipsilateral and contralateral to the epileptic focus.
* For difference in mean count between the ipsilateral and contralateral sides.

patients by means of IMZ-SPECT. Interhemispheric comparison revealed significant decreases in IMZ activity in the hemisphere ipsilateral to the epileptic focus, not only in the anterior and mesial temporal lobe but also in extratemporal regions.

To analyze altered IMZ activity in MTLE patients, we investigated asymmetry of IMZ uptake between hemispheres ipsilateral and contralateral to the epileptic focus. Two different methods, VB analysis with SPM and VOI analysis with 3D-SSP, were applied. VB analysis automatically shows areas of statistical significance in the whole brain. VOI analysis by 3D-SSP with predefined VOIs is also fully automatic. Manual delineation of regions of interest (ROIs) is widely used in comparative imaging. However, it is difficult to place ROIs manually on SPECT images because of the low spatial resolution. Thus, we used two more objective methods, VB and VOI analyses, in this study.

For our multi-subject analyses, brains were normalized into a standard brain space. VB statistical analysis with SPM can analyze the whole brain exhaustively and can evaluate the detailed extent of abnormalities on a voxel or cluster level. Such statistical voxel-based analysis was established by Friston et al. (1995a,b) and later applied in many studies. The VOI analysis uses a predefined set of VOIs on the standard stereotactic space of the Talairach atlas to eliminate rater-dependent bias (Hosoda et al., 2005; Takada et al., 2006). Spatial normalization with 3D-SSP, which was applied before calculation of the average counts in VOIs, has a particular advantage in the atrophic brain (Ishii et al., 2001).

The VB and VOI data represented intra-individual differences and relative interhemispheric asymmetry. Interhemispheric asymmetry analysis has been widely applied in both research and clinical settings (Kim et al., 2003; Aubert-Broche et al., 2005; Hammers et al., 2008; Didelot et al., 2010). Interhemispheric asymmetry analysis of FDG-PET images correctly detected the epileptic zone in 69% of patients in whom simple comparisons revealed no significant or bilateral temporal hypometabolism (Kim et al., 2003); this analysis was also thought to reduce the false-positive findings and correctly identify true-positive findings (Hammers et al., 2008). Moreover, these methods can be applied without a normal control group, can evaluate regions of low IMZ activity, and may be acceptable for analysis with qualitative images. Six of our 14 patients were taking benzodiazepines, which can partially block binding of IMZ. The interhemispheric asymmetry analysis makes results interpretable in such cases. In line with these reported applications, we analyzed interhemispheric asymmetry of IMZ uptake in our patients.

To analyze all data from all 14 of our patients together, the IMZ-SPECT images obtained from the 6 patients with left MTLE were left-right flipped, as previously reported (Kim et al., 2003; Hammers et al., 2008). The side of the epileptic focus and the exact histologic diagnosis were confirmed in each patient on the basis of the post-surgical outcomes.

The late IMZ-SPECT images are thought to correspond to retention of the tracer at specific cBZR binding sites, and the early images are thought to depict both regional CBF and cBZR density (Beer et al., 1990; Schubiger et al., 1991; Tanaka et al., 1997). When we use FMZ-PET, measuring the arterial input function is important to accurately determine cBZR density with adequate exclusion of the regional variations in cerebral blood flow (CBF) (Hammers et al., 2008). Because of the long half-life of IMZ tracer, we can easily obtain late Images 3 h after injection. Therefore, we relied on the late images reflecting cBZR density without measuring arterial input function.

Please cite this article in press as: Hosomi, K., et al., Altered extrafocal iomazenil activity in mesial temporal lobe epilepsy. Epilepsy Res. (2012), http://dx.doi.org/10.1016/j.eplepsyres.2012.07.001

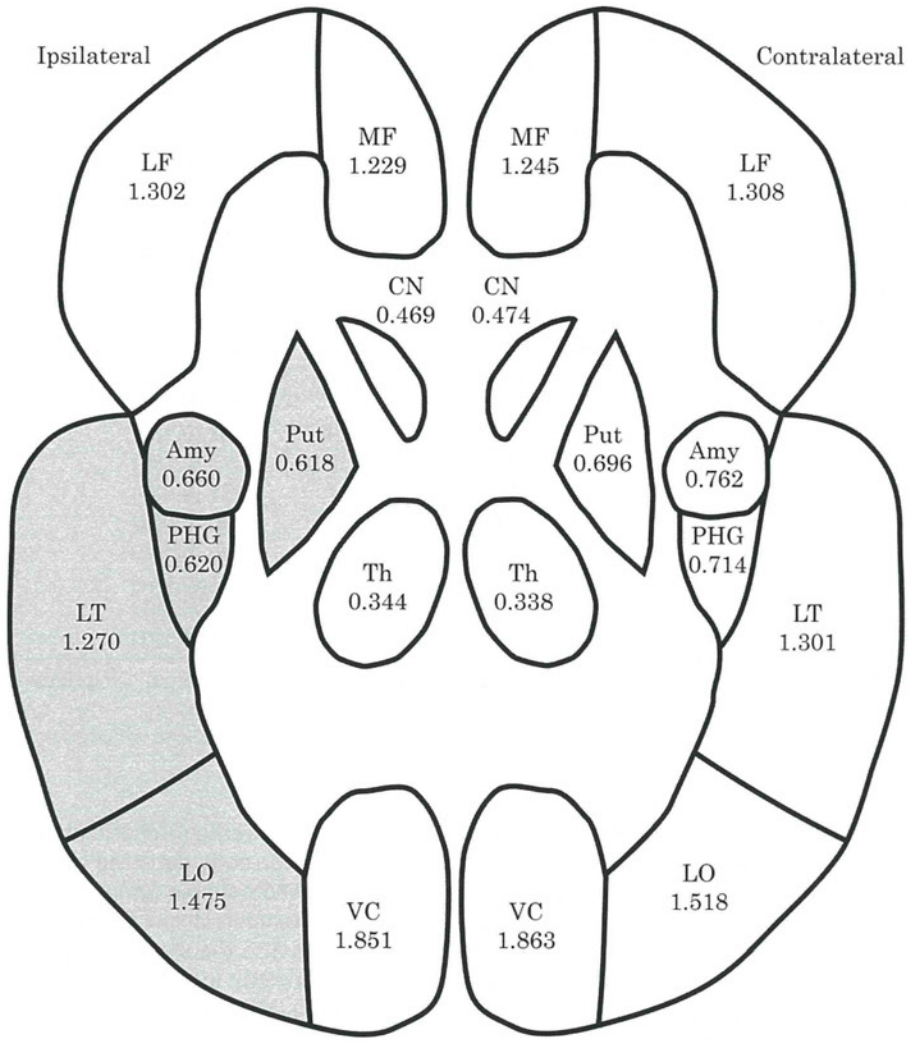

Figure 2 Schematic drawing of the topography of each average count. The ipsilateral gray regions have significantly lower counts than those on the contralateral side. Each mean corrected count is shown for each region. LF, lateral frontal lobe; MF, medial frontal lobe; LT, lateral temporal lobe; LO, lateral occipital lobe; VC, primary visual cortex; Amy, amygdala; PHG, parahippocampal gyrus; CN, caudate nucleus; Put, putamen; Th, thalamus.

We performed only group analysis in this study. If a normal control set or thresholds of normal asymmetry become available, further individual analysis could be performed. Such analysis might be useful for clinical diagnosis in individual patients and pathophysiologic consideration of individual symptoms.

Abnormalities in the temporal lobe

VB analysis showed that the most significant decreases in IMZ binding extended widely from the medial part to the temporal tip and lateral part of the anterior temporal lobe. VOI analysis also showed significant decreases in the parahippocampal gyrus, amygdala, and lateral temporal cortex. Previous FMZ-PET studies, using SPM for individual and group analyses, have depicted reduction of cBZR binding in the ipsilateral hippocampus in MTLE patients with unilateral hippocampal sclerosis (Koepp et al., 1996; Hammers et al., 2001) and the TLE patients without MRI abnormalities (Koepp et al., 2000; Hammers et al., 2002). Other previous studies revealed histologic, morphologic, or functional abnormalities not only in the medial part of the temporal lobe, including the hippocampus, but also in the tip and lateral cortex of the temporal lobe ipsilateral to the epileptic focus in patients with MTLE (Semah et al., 1995; Coste et al., 2002; Cendes et al., 2005). Our finding of the anterior temporal lobe abnormality extending beyond the mesial temporal structure is consistent with these previously reported findings. Satisfactory surgical outcomes were achieved in 13 of our 14 patients by means of selective amygdalohippocampectomy without anterior temporal lobectomy, suggesting that regions of the anterior temporal lobe outside the amygdala, hippocampus, and parahippocampal gyrus are not likely to be the epileptic foci of MTLE, even if they are characterized by decreased IMZ activity.

The exact role played by decreased cBZR in this region is not clear. Lack of correlation between cBZR density and neuronal density on volumetric MRI prompted Koepp et al. (1997) to conclude that atrophy with neuronal loss is not the

Please cite this article in press as: Hosomi, K., et al., Altered extrafocal iomazenil activity in mesial temporal lobe epilepsy. Epilepsy Res. (2012), http://dx.doi.org/10.1016/j.eplepsyres.2012.07.001

sole determinant of reduced cBZR binding in patients with MTLE. Decreased cBZR density is thought to reflect impaired GABAergic transmission as well as neuronal loss.

Abnormalities in extratemporal regions

In our study, significant decreases in IMZ bindings extended to extratemporal regions ipsilateral to the side of seizure onset. By VB analysis, significant decreases were detected in the insula and basal ganglia and in the medial cortices of the occipital lobe. Similarly, VOI analysis showed significant decreases in the putamen and the lateral occipital cortex. The extratemporal abnormalities we found by the two different methods shed some light on the pathology of MTLE. In line with our results, previous FMT-PET studies have reported altered extrafocal cBZR distribution in individual patients with MTLE (Hammers et al., 2001; Bouilleret et al., 2002) and neocortical partial epilepsy (Juhasz et al., 2009). Moreover, decreased extrafocal serotonin receptor density has recently been reported in individual patients with MTLE (Didelot et al., 2010). An MRI study that tracked the progression of neocortical atrophy associated with TLE revealed progressive cortical atrophy in various extratemporal lobes (Bernhardt et al., 2009). These extrafocal abnormalities likely represent seizure-induced cortical damage.

Decreased IMZ activity in the insula and the basal ganglia may be the result of direct abnormal neuronal transmission propagated from the primary epileptic focus. The insula is related to generation of the abdominal aura and epigastric discomfort (Isnard et al., 2004) experienced by patients with MTLE. The basal ganglia are thought to be involved in the generation of ictal dystonic posturing (Dupont et al., 1998) and secondarily generalized tonic-clonic seizures (Blumenfeld et al., 2009). Extratemporal glucose hypometabolism in the ipsilateral insula has been reported in patients with MTLE (Wong et al., 2010). Another group detected highly significant hypometabolism and decreased cBZR in the insular cortices of patients with MTLE (Bouilleret et al., 2002); furthermore, the insular hypometabolism did not influence outcomes after anterior temporal lobectomy. Most of our study patients experienced abdominal auras, some showed contralateral dystonic posturing, and all obtained a satisfactory outcome after surgery. Therefore, decreased IMZ activity in the insula and basal ganglia is not necessarily indicative of secondary epileptic foci.

A decrease in IMZ activity was also revealed in the ipsilateral occipital lobe by both VB and VOI analyses. Various extratemporal neocortices are reported to be abnormal or functionally impaired in patients with MTLE (Cendes et al., 2005). Several FDG-PET-based studies have shown that various neocortices, including the occipital lobe, can exist as functional deficit zones (Henry et al., 1990; Arnold et al., 1996; Wong et al., 2010). Wong et al. (2010) reported ipsilateral glucose hypometabolism in the medial and lateral occipital lobe in patients with MTLE. The occipital decrease in IMZ bindings in our study patients is consistent with this finding. A white matter associative tract connecting the temporal and occipital lobes is known as the inferior longitudinal fasciculus. A diffusion tensor imaging study showed direct connections between the temporal and occipital lobe. The temporal branches start at the parahippocampal gyrus, amygdala and lateral temporal cortex, and the occipital branches terminate at the lateral and medial occipital cortex (Catani et al., 2003). This connection, which allows propagation of abnormal epileptogenic discharges, may be affected by the occipital decrease we observed.

In conclusion, the data yielded by our VB and VOI analyses of interhemispheric IMZ activity indicate that destructive inhibitory dysfunction spreads from the mesial temporal lobe to the anterior temporal lobe and extends to basal ganglia, insula, and occipital lobe in patients with MTLE. We expect these findings, along with further individual investigations, to contribute to understanding of the pathophysiology of seizure propagation and to the diagnosis of MTLE.

Disclosure of conflicts of interest

None of the authors has any conflict of interest to disclose. We confirm that we have read the Journal's position on issues involved in ethical publication and affirm that this report is consistent with those guidelines.

Acknowledgment

This work was supported in part by a Grant-in-Aid for Scientific Research (21591869) from the Ministry of Education, Culture, Sports, Science and Technology of Japan.

References

Arnold, S., Schlaug, G., Niemann, H., Ebner, A., Luders, H., Witte, O.W., Seitz, R.J., 1996. Topography of interictal glucose hypometabolism in unilateral mesiotemporal epilepsy. Neurology 46, 1422–1430.

Aubert-Broche, B., Jannin, P., Biraben, A., Bernard, A.M., Haegelen, C., Le Jeune, F.P., Gibaud, B., 2005. Evaluation of methods to detect interhemispheric asymmetry on cerebral perfusion SPECT: application to epilepsy. J. Nucl. Med. 46, 707–713.

Beer, H.F., Blauenstein, P.A., Hasler, P.H., Delaloye, B., Riccabona, G., Bangerl, I., Hunkeler, W., Bonetti, E.P., Pieri, L., Richards, J.G., Schubiger, P.A., 1990. In vitro and in vivo evaluation of iodine-123-Ro 16-0154: a new imaging agent for SPECT investigations of benzodiazepine receptors. J. Nucl. Med. 31, 1007–1014.

Bernhardt, B.C., Worsley, K.J., Kim, H., Evans, A.C., Bernasconi, A., Bernasconi, N., 2009. Longitudinal and cross-sectional analysis of atrophy in pharmacoresistant temporal lobe epilepsy. Neurology 72, 1747–1754.

Blumenfeld, H., Varghese, G.I., Purcaro, M.J., Motelow, J.E., Enev, M., McNally, K.A., Levin, A.R., Hirsch, L.J., Tikofsky, R., Zubal, I.G., Paige, A.L., Spencer, S.S., 2009. Cortical and subcortical networks in human secondarily generalized tonic-clonic seizures. Brain 132, 999–1012.

Bouilleret, V., Dupont, S., Spelle, L., Baulac, M., Samson, Y., Semah, F., 2002. Insular cortex involvement in mesiotemporal lobe epilepsy: a positron emission tomography study. Ann. Neurol. 51, 202–208.

Brett, M., Johnsrude, I.S., Owen, A.M., 2002. The problem of functional localization in the human brain. Nat. Rev. Neurosci. 3, 243–249.

Catani, M., Jones, D.K., Donato, R., Ffytche, D.H., 2003. Occipito-temporal connections in the human brain. Brain 126, 2093–2107.

Please cite this article in press as: Hosomi, K., et al., Altered extrafocal iomazenil activity in mesial temporal lobe epilepsy. Epilepsy Res. (2012), http://dx.doi.org/10.1016/j.eplepsyres.2012.07.001

Cendes, F., Kahane, P., Brodie, M., Andermann, F., 2005. The mesiotemporal lobe epilepsy syndrome. In: Roger, J., Bureau, M., Dravet, C., Genton, P., Tassinari, C.A., Wolf, P. (Eds.), Epileptic Syndromes in Infancy, Childhood and Adolescence. John Libbey Eurotext Ltd., Montrouge, pp. 555–578.

Coste, S., Ryvlin, P., Hermier, M., Ostrowsky, K., Adeleine, P., Froment, J.C., Mauguiere, F., 2002. Temporopolar changes in temporal lobe epilepsy: a quantitative MRI-based study. Neurology 59, 855–861.

Didelot, A., Mauguiere, F., Redoute, J., Bouvard, S., Lothe, A., Reilhac, A., Hammers, A., Costes, N., Ryvlin, P., 2010. Voxel-based analysis of asymmetry index maps increases the specificity of 18F-MPPF PET abnormalities for localizing the epileptogenic zone in temporal lobe epilepsies. J. Nucl. Med. 51, 1732–1739.

Dupont, S., Semah, F., Baulac, M., Samson, Y., 1998. The underlying pathophysiology of ictal dystonia in temporal lobe epilepsy: an FDG-PET study. Neurology 51, 1289–1292.

Engel Jr., J., Van Ness, P.C., Rasmussen, T., Ojemann, L.M., 1993. Outcome with respect to epileptic seizures. In: Engel Jr., J. (Ed.), Surgical Treatment of the Epilepsies. Raven Press, New York, pp. 609–622.

Friston, K.J., Ashburner, J., Poline, J.B., Frith, C.D., Heather, J.D., Frackowiak, R.S., 1995a. Spatial registration and normalization of images. Hum. Brain Mapp. 2, 165–189.

Friston, K.J., Holmes, A.P., Worsley, K.J., Poline, J.B., Frith, C.D., Frackowiak, R.S., 1995b. Statistical parametric maps in functional imaging: a general linear approach. Hum. Brain Mapp. 2, 189–210.

Hammers, A., Koepp, M.J., Labbe, C., Brooks, D.J., Thom, M., Cunningham, V.J., Duncan, J.S., 2001. Neocortical abnormalities of [^{11}C]-flumazenil PET in mesial temporal lobe epilepsy. Neurology 56, 897–906.

Hammers, A., Koepp, M.J., Hurlemann, R., Thom, M., Richardson, M.P., Brooks, D.J., Duncan, J.S., 2002. Abnormalities of grey and white matter [^{11}C]flumazenil binding in temporal lobe epilepsy with normal MRI. Brain 125, 2257–2271.

Hammers, A., Panagoda, P., Heckemann, R.A., Kelsch, W., Turkheimer, F.E., Brooks, D.J., Duncan, J.S., Koepp, M.J., 2008. [^{11}C]Flumazenil PET in temporal lobe epilepsy: do we need an arterial input function or kinetic modeling? J. Cereb. Blood Flow Metab. 28, 207–216.

Heinzel, A., Steinke, R., Poeppel, T.D., Grosser, O., Bogerts, B., Otto, H., Northoff, G., 2008. S-ketamine and GABA-A-receptor interaction in humans: an exploratory study with I-123-iomazenil SPECT. Hum. Psychopharmacol. 23, 549–554.

Henry, T.R., Mazziotta, J.C., Engel Jr., J., Christenson, P.D., Zhang, J.X., Phelps, M.E., Kuhl, D.E., 1990. Quantifying interictal metabolic activity in human temporal lobe epilepsy. J. Cereb. Blood Flow Metab. 10, 748–757.

Hosoda, K., Kawaguchi, T., Ishii, K., Minoshima, S., Kohmura, E., 2005. Comparison of conventional region of interest and statistical mapping method in brain single-photon emission computed tomography for prediction of hyperperfusion after carotid endarterectomy. Neurosurgery 57, 32–41.

Ishii, K., Willoch, F., Minoshima, S., Drzezga, A., Ficaro, E.P., Cross, D.J., Kuhl, D.E., Schwaiger, M., 2001. Statistical brain mapping of 18F-FDG PET in Alzheimer's disease: validation of anatomic standardization for atrophied brains. J. Nucl. Med. 42, 548–557.

Isnard, J., Guenot, M., Sindou, M., Mauguiere, F., 2004. Clinical manifestations of insular lobe seizures: a stereo-electroencephalographic study. Epilepsia 45, 1079–1090.

Johnson, E.W., de Lanerolle, N.C., Kim, J.H., Sundaresan, S., Spencer, D.D., Mattson, R.H., Zoghbi, S.S., Baldwin, R.M., Hoffer, P.B., Seibyl, J.P., Innis, R.B., 1992. ''Central'' and ''peripheral'' benzodiazepine receptors: opposite changes in human epileptogenic tissue. Neurology 42, 811–815.

Juhasz, C., Asano, E., Shah, A., Chugani, D.C., Batista, C.E., Muzik, O., Sood, S., Chugani, H.T., 2009. Focal decreases of cortical GABAA receptor binding remote from the primary seizure focus: what do they indicate? Epilepsia 50, 240–250.

Kaneko, K., Sasaki, M., Morioka, T., Koga, H., Abe, K., Sawamoto, H., Ohya, N., Yoshiura, T., Mihara, F., Honda, H., 2006. Presurgical identification of epileptogenic areas in temporal lobe epilepsy by ^{123}I-iomazenil SPECT: a comparison with IMP SPECT and FDG PET. Nucl. Med. Commun. 27, 893–899.

Kim, Y.K., Lee, D.S., Lee, S.K., Kim, S.K., Chung, C.K., Chang, K.H., Choi, K.Y., Chung, J.K., Lee, M.C., 2003. Differential features of metabolic abnormalities between medial and lateral temporal lobe epilepsy: quantitative analysis of (18)F-FDG PET using SPM. J. Nucl. Med. 44, 1006–1012.

Kimura, K., Hashikawa, K., Etani, H., Uehara, A., Kozuka, T., Moriwaki, H., Isaka, Y., Matsumoto, M., Kamada, T., Moriyama, H., Tabuchi, H., 1990. A new apparatus for brain imaging: four-head rotating gamma camera single-photon emission computed tomograph. J. Nucl. Med. 31, 603–609.

Koepp, M.J., Richardson, M.P., Brooks, D.J., Poline, J.B., Van Paesschen, W., Friston, K.J., Duncan, J.S., 1996. Cerebral benzodiazepine receptors in hippocampal sclerosis. An objective in vivo analysis. Brain 119, 1677–1687.

Koepp, M.J., Richardson, M.P., Labbe, C., Brooks, D.J., Cunningham, V.J., Ashburner, J., Van Paesschen, W., Revesz, T., Duncan, J.S., 1997. ^{11}C-flumazenil PET, volumetric MRI, and quantitative pathology in mesial temporal lobe epilepsy. Neurology 49, 764–773.

Koepp, M.J., Hammers, A., Labbe, C., Woermann, F.G., Brooks, D.J., Duncan, J.S., 2000. ^{11}C-flumazenil PET in patients with refractory temporal lobe epilepsy and normal MRI. Neurology 54, 332–339.

Kugaya, A., Sanacora, G., Verhoeff, N.P., Fujita, M., Mason, G.F., Seneca, N.M., Bozkurt, A., Khan, S.A., Anand, A., Degen, K., Charney, D.S., Zoghbi, S.S., Baldwin, R.M., Seibyl, J.P., Innis, R.B., 2003. Cerebral benzodiazepine receptors in depressed patients measured with [^{123}I]iomazenil SPECT. Biol. Psychiatry 54, 792–799.

Kurokawa, K., Jibiki, I., Matsuda, H., Fukushima, T., Tsuji, S., Yamaguchi, N., Hisada, K., 1994. Comparison of benzodiazepine receptor and regional cerebral blood flow imaging of epileptiform foci in hippocampal kindled rabbits: a study with in vivo double tracer autoradiography using ^{125}I-iomazenil and 99mTc-HMPAO. Brain Res. 642, 303–310.

Minoshima, S., Koeppe, R.A., Frey, K.A., Kuhl, D.E., 1994. Anatomic standardization: linear scaling and nonlinear warping of functional brain images. J. Nucl. Med. 35, 1528–1537.

Minoshima, S., Frey, K.A., Koeppe, R.A., Foster, N.L., Kuhl, D.E., 1995. A diagnostic approach in Alzheimer's disease using three-dimensional stereotactic surface projections of fluorine-18-FDG PET. J. Nucl. Med. 36, 1238–1248.

Schubiger, P.A., Hasler, P.H., Beer-Wohlfahrt, H., Bekier, A., Oettli, R., Cordes, M., Ferstl, F., Deisenhammer, E., De Roo, M., Moser, E., Nitzsche, E., Podreka, I., Riccabona, G., Bangerl, I., Schober, O., Bartenstein, P., Van Rijk, P., Van Isselt, J.W., Van Royen, E.A., Verhoeff, N.P., Haldemann, R., Von Schulthess, G.K., 1991. Evaluation of a multicentre study with Iomazenil – a benzodiazepine receptor ligand. Nucl. Med. Commun. 12, 569–582.

Semah, F., Baulac, M., Hasboun, D., Frouin, V., Mangin, J.F., Papageorgiou, S., Leroy-Willig, A., Philippon, J., Laplane, D., Samson, Y., 1995. Is interictal temporal hypometabolism related to mesial temporal sclerosis? A positron emission tomography/magnetic resonance imaging confrontation. Epilepsia 36, 447–456.

Takada, S., Yoshimura, M., Shindo, H., Saito, K., Koizumi, K., Utsumi, H., Abe, K., 2006. New semiquantitative assessment of ^{123}I-FP-CIT by an anatomical standardization method. Ann. Nucl. Med. 20, 477–484.

Talairach, J., Tournoux, P., 1988. Co-planar Stereotaxic Atlas of the Human Brain. Thieme, New York.

Please cite this article in press as: Hosomi, K., et al., Altered extrafocal iomazenil activity in mesial temporal lobe epilepsy. Epilepsy Res. (2012), http://dx.doi.org/10.1016/j.eplepsyres.2012.07.001